Original Research Report

Effects of the Implant Design on Peri-implant Bone Stress and Abutment Micromovement: Three-Dimensional Finite Element Analysis of Original Computer-Aided Design Models

Yasufumi Yamanishi, PhD[*†], Satoshi Yamaguchi, PhD*, Satoshi Imazato, PhD[*], Tamaki Nakano, PhD[†], Hirofumi Yatani, PhD[†]

[*]Department of Biomaterials Science, Osaka University Graduate School of Dentistry, Osaka, Japan

[†]Department of Fixed Prosthodontics, Osaka University Graduate School of Dentistry, Osaka, Japan

Short Title: Effects of the design of the implant

Corresponding author: Satoshi Yamaguchi, PhD, Department of Biomaterials Science, Osaka University Graduate School of Dentistry, 1-8 Yamadaoka, Suita 565-0871, Japan.

Tel: +81-6-6879-2919; Fax: +81-6-6879-2919; E-mail: yamagu@dent.osaka-u.ac.jp

Conflict of interest: None

[This study revealed the effect of the implant's design on peri-implant bone stress and abutment micromovement using original CAD models focused on specific differences between implants.]

Abstract

Background: Occlusal overloading causes peri-implant bone resorption. Previous studies examined stress distribution in alveolar bone around commercial implants using three-dimensional finite element analysis (3D-FEA). However, commercial implants contained some different designs and it has been impossible to determine the effect of particular design. The purpose of this study was to reveal the effect of the target design on peri-implant bone stress and abutment micromovement using original computer-aided design (CAD) models.

Methods: Six 3D implant models were created for different implant-abutment joints: external and internal models (EM, IM); straight and tapered abutment shapes (SA, TA); platform switching (PS) in the IM; modified TA neck design [reverse conical neck (RN)]. “Contact” conditions were set at the component interface. A static load of 100 N was applied to the basal ridge surface of the abutment at a 45° oblique angle to the long axis of the implant. (1) Stress distribution in peri-implant bone, (2) abutment micromovement in SA and TA models were analyzed.

Results: Compressive stress concentrated on labial cortical bone and tensile stress on the palatal side in the EM and on the labial side in the IM. There was no difference in maximum principal stress distribution for SA and TA models. Tensile stress

concentration was not apparent on labial cortical bone in the PS model (versus IM). Maximum principal stress concentrated more on peri-implant bone in the RN than in the TA model. TA model exhibited less abutment micromovement than the SA model.

Conclusions: Internal joint types are more suitable than external joint types regarding occlusal overloading. Platform switching decreases compressive stress on labial bone. Reverse conical neck types increase peri-implant bone stress. Tapered abutments decrease abutment micromovement, but do not influence maximum principal stress on peri-implant bone.

KEYWORDS: biomechanics, dental implant, finite element analysis, occlusal overloading, micromovement

Introduction

In accordance with their increased success rate, dental implants have become a popular treatment option for missing teeth. One of the criteria for a successful dental implant is radiographically visualized vertical peri-implant bone loss of <2.0 mm.[1] Remodeling of peri-implant bone occurs once the implant is exposed to the oral environment by a second surgical procedure or immediate placement of an abutment after implant surgery. Several factors negatively affect the remodeling process and result in marginal bone resorption. They include traumatic surgical technique,[2] excessive loading conditions,[3] microbial contamination of the microgap between an implant and an abutment,[4-6] micromovement of an implant and abutment,[4,7-9] and repeated screwing and unscrewing.[10] Exclusion of one or more of these factors is important for a successful implant.

Osteoclastic bone resorption occurs in areas where microcracks are produced by occlusal dynamic stress and osteocyte apoptosis.[11,12] The threshold values of tensile and shear stresses that cause resorption of cortical bone have been reported to be, respectively, about 30% and 65% more than the threshold value of compressive stress.[13,14] It has been also demonstrated that peri-implant bone resorption can be

effectively controlled by reducing the shear stress caused by occlusal loading.[14] Considering the benefits of eliminating an excessive occlusal loading condition,[15-20] much attention has been paid to biomechanical evaluation of implants. Finite element analysis (FEA) is useful for numerical stress analysis of multiple structured materials and has been widely used to analyze dental implants.[17-19] However, in most previous FEA studies, the individual geometries of the commercially available implants were transferred to three-dimensional (3D) finite element (FE) models.[21] Although these transferred models are clinically relevant, the designs of the components of commercial implants may differ. Therefore, the effect of a specific difference (e.g., the taper of the abutment) in an implant design on peri-implant bone stress has not been evaluated.

Previous studies have reported that severe peri-implant bone resorption was found around two-piece implants because of abutment micromovement and microgap formation between the implant and the abutment.[4,8,9] In addition to the negative effects on peri-implant bone remodeling,[22] abutment micromovement may also induce destruction of the epithelial attachment to the abutment and crown and result in bacterial microleakage.[10,23] However, it has been impossible to measure micromovement and microgap in vivo, so in vitro studies have been conducted.[23] Thus, one of the purposes

of the current study was to simulate abutment micromovement and assess the effect of the taper of the abutment during the micromovement in 3D two-piece implant CAD models.

In this study, we focused on specific differences between implants using the CAD models. The purpose of this study was to reveal the effect of the implant's design on peri-implant bone stress and abutment micromovement using 3D FEA evaluation of the two-piece structured implant models.

Materials and Methods

3D CAD Model

Six 3D computer-aided design (CAD) models were created by SolidWorks software (SolidWorks Premium 2012; SolidWorks Corporation, Waltham, MA, USA) (Fig. 1). Implant–abutment joints were prepared to investigate the influence of different designs: external joint (EM) and internal joint (IM) models; different shapes of the abutment: straight abutment (SA) and tapered abutment (TA) models; addition of platform switching to the IM model (PS model); and modifying the neck design of the TA model to become a reverse conical neck (RN model). Each model had the same shape and size. Their only difference was the single alteration in one component of the model. The diameter and length of the implant body was φ5×13 mm, and the pitch of the threads was 0.9 mm. The shape of the threads and abutment screw were the same in all models. The diameter and length of the abutment screw that connected the implant and the abutment was φ1.5×11 mm.

Each 3D implant model was placed in a 3D CAD anterior maxillary model with 1.5 mm thick cortical bone (top side 9×9 mm) and cancellous bone (Fig. 2A). The mechanical properties of the bone and titanium used for the FE models are shown in Table 1.[24] For

simulations of osseointegrated implants, a “fixed bond” condition was set at the interface of the bone and the implant. A “contact” condition that accepts possible microscopic sliding was set at the interfaces of the components of the implants. The bottom part of the maxillary bone and both sectional surfaces of the bone segment were fixed.

Peri-implant Bone Stress

A static load of 100 N was applied to the basal ridge surface of the abutment at a 45° oblique angle to the long axis of the implant (Fig. 2B). Distribution of the maximum principal stress in the peri-implant bone was assessed. The distribution of the maximum principal stress in the cortical bone was evaluated in the middle section of the mesiodistal plane. The elements for FEA were tetrahedrons with 16 nodes. To determine the optimal mesh size that offered reliable results within a reasonable computational cost (<15 minutes), the number of elements was increased until the maximum principal stress converged. The results of convergence analysis are shown in Fig. 3. The total number of elements for each model were 42,992 (EM), 42,714 (IM), 42,849 (SA), 34,786 (TA), 41,231 (PS), and 41,380 (RN). FEA was performed by SolidWorks Premium 2012 software (SolidWorks Corporation).

Abutment Micromovement

Abutment displacement distribution was assessed as micromovement. In our previous study,[25] we confirmed that the taper of the abutment contributed to reducing abutment micromovement. Therefore, abutment displacement distribution in the SA model was qualitatively compared with that of the TA model in the mesiodistal plane.

Results

Peri-implant Bone Stress

Figure 4 shows the maximum principal stress distribution in the mesiodistal half of the peri-implant bone. The red areas indicate the tensile stress (positive value of the maximum principal stress) and the blue areas the compressive stress (negative value of maximum principal stress). Compressive stress concentrated on the labial side of the cortical bone and tensile stress on the palatal side in the EM model. In the IM model, compressive stress concentrated on the labial side. There was no difference in the maximum principal stress distribution in peri-implant bone in the SA and TA models. Compared with the IM model, the concentration of the compressive stress in the PS model was decreased on the labial side of the cortical bone. Also, more tensile stress

concentrated on not only the labial side but also the mesiodistal side of the peri-implant bone in the RN model than in the SA model.

Abutment Micromovement

Figure 5 shows the displacement distribution of the abutment for the TA and SA models. The maximum abutment displacements for the SA and TA models were 0.029 mm and 0.014 mm, respectively. For the SA model, the vector was expressed in a negative direction between the x-axis and z-axis. For the TA model, a sum of the displacement vectors was mostly directed in a negative direction on the z-axis.

Discussion

The designs of commercially available implants may differ (e.g., their diameters, thread pitches, abutment tapering). Therefore, it has been impossible to determine the effect the target design of implants may have on peri-implant bone stress in studies focusing on single components of commercial implants using FE models and a 3D scanner. In the present study, we created 3D CAD models that restricted the difference in implant design to a single alteration in each model to evaluate the effect of the particular design change on peri-implant bone stress.

Depending on the solidity of a food, the average bite force ranges from 20 to 120 N.[26] In the present study, we applied a static load of 100 N to simulate an occlusive load, in reference to some previous studies.[27,28] The maximum principal stress concentration in the bone with the two-piece implant occurred around the neck, similar to the results of previous reports that demonstrated concentrations of various stresses (e.g., von Mises stress, compressive stress, tensile stress, and shear stress) around the neck of one-piece implant models.[17-19,27] Thus, with the two-piece implant, the abutment screw creates a solid connection between the implant body and the abutment.

Regarding implant–abutment joints, the tensile stress was less concentrated in the IM model than in the EM model, and the boundary between compressive and tensile stresses was clearly shown on the mesiodistal side of the cortical bone. This result indicates that the shear stress on peri-implant bone in the direction of the z-axis was concentrated on the mesiodistal side of the cortical bone in the EM model.[25] It suggests that the deep, rigid connections of internal joint implants are less sensitive to stress distribution and transmit the load more directly to the labial side of the cortical bone. In contrast, the flexible connections of external joint implants transmit the load to both the

labial and palatal sides of cortical bone. Thus, internal joint implants have a biomechanical advantage over external joint implants regarding implant-supported single restoration. In a previous study with radiographic evidence, peri-implant crestal bone resorption was significantly greater in the external joint than in the internal joint.[29]

A clinical study that investigated radiographic records retrospectively demonstrated that platform switching effectively minimized marginal bone loss.[30] The maximum principal stress on peri-implant bone was less concentrated on the labial side of the cortical bone in the PS model than in the IM model. Hence, platform switching effectively reduces peri-implant bone stress. It is therefore considered that platform switching is helpful for preserving peri-implant bone.

Comparing the design of the neck of implants in the RN and TA models, the tensile stress was more concentrated on the peri-implant bone in the RN model than in the TA model. It is thought that reverse conical neck implants are disadvantageous in regard to preservation of labial bone, possibly because it is believed that reverse conical neck implants are more technique-sensitive,[31, 32] and the implant position requires exquisite care to prevent the peri-implant bone resorption.

Regarding abutment shape, the maximum principal stress distribution around the neck of the implants showed no difference between the SA and TA models, indicating that the taper of the abutment has no effect on peri-implant bone resorption.[25] In a clinical radiographic study, the tapered internal implant had no significant effect on crestal bone resorption,[32] suggesting that the design of the implant's neck has a greater effect on peri-implant bone stress than does the shape of the abutment.

We carefully evaluated the effect of the shape of the abutment on abutment displacement and found that abutment micromovement was less in the TA model than in the SA model. A previous FEA study with commercially available implant models suggested that the tapered abutment resisted microscopic sliding between the implant and the abutment.[25] There was no difference in the abutment displacement distribution among the models[25] because of multiple effects caused by different designs (e.g., diameters and lengths of the implant bodies, implant–abutment joints, neck designs of the implants). The present study demonstrated that the taper of the abutment reduces the abutment micromovement when compared to that in the SA and TA models, with the difference restricted to the abutment design.

In the present study, the 3D CAD models with singular differences in design were useful for evaluating effects strictly related to peri-implant bone stress and the implants' components in three dimensions. One of the limitations of this study was a lack of simulation of the inhomogeneous and anisotropic material properties of human bone. Although our results with homogeneous and isotropic material properties definitively clarified the effect of implant designs on peri-implant bone stress and abutment micromovement, further analysis is required with detailed simulation of a more realistic bone model and some clinical cases. Selecting the best implant design for each clinical situation may help exclude overload and so achieve a better prognosis.

Conclusions

We used CAD models to investigate different structures of implants. The study revealed the effects of the design of specific components on peri-implant bone stress and abutment displacement after implant-supported single restoration in the anterior maxilla. Within the limitations of an FEA study, the following conclusions were drawn: (1) biomechanically, internal joint types are more suitable than external joint types; (2) the use of tapered abutments decreases abutment micromovement; (3) platform switching

decreases compressive stress on the labial bone; and (4) reverse conical neck implants increase peri-implant bone stress.

Acknowledgment

This research was supported by a Grant-in-Aid for Scientific Research (No. 24592955) from the Japan Society for the Promotion of Science.

References

1. Misch CE, Perel ML, Wang HL, et al. Implant success, survival, and failure: the International Congress of Oral Implantologists (ICOI) Pisa Consensus Conference. *Implant Dent* 2008;17:5-15.

2. Becker W, Goldstein M. Minimally invasive flapless implant surgery: a prospective multicenter study. *Clin Implant Dent Relat Res* 2005;7(Suppl 1):S21-S27.

3. Kim Y, Oh TJ. Occlusal considerations in implant therapy: clinical guidelines with biomechanical rationale. *Clin Oral Implants Res* 2005;16:26-35.

4. Hermann JS, Schoolfield JD. Influence of the size of the microgap on crestal bone changes around titanium implants: a histometric evaluation of unloaded non-submerged implants in the canine mandible. *J Periodontol* 2001;72:1372-1383.

5. Weng D, Nagata MJ. Influence of microgap location and configuration on the periimplant bone morphology in submerged implants: an experimental study in dogs. *Clin Oral Implants Res* 2008;19:1141-1147.

6. Ericsson I, Persson LG. Different types of inflammatory reactions in peri-implant soft tissues. *J Clin Periodontol* 1995;22:255-261.

7. King GN, Hermann JS. Influence of the size of the microgap on crestal bone levels in non-submerged dental implants: a radiographic study in the canine mandible. *J Periodontol* 2002;73:1111-1117.

8. Weng D, Nagata MJH, Bosco AF, Melo LGN. Influence of microgap location and configuration on radiographic bone loss around submerged implants: an experimental study in dogs. *Int J Oral Maxillofac Implants* 2011;26:941-946.

9. Hermann JS, Schoolfield JD, Scenk RK, Buser D, Cochran DL. Influence of the size of the microgap on crestal bone changes around titanium implants: a histometric evaluation of unloaded non-submerged implants in the canine mandible. *J Periodontol* 2001;72:1372-1383.

10. Abrahamsson I, Berglundh T. The mucosal barrier following abutment dis/reconnection: an experimental study in dogs. *J Clin Periodontol* 1997;24:568-572.

11. Verborgt O, Gibson GJ, Schaffler MB. Loss of osteocyte integrity in association

with microdamage and bone remodeling after fatigue in vivo. *J Bone Miner Res* 2000;15:60-67.

12. Huiskes R, Ruimerman R. Effect of mechanical forces on maintenance and adaptation of form in trabecular bone. *Nature* 2000;405:704-706.

13. Reilly DT, Burstein AH. The elastic and ultimate properties of compact bone tissue. *J Biomech* 1975;8:393-405.

14. Guo XE. Mechanical properties of cortical bone and cancellous bone tissue. In: Cowin SC, ed. *Bone Mechanics Handbook*. Boca Raton, FL: CRC Press; 2001:1-23.

15. Schrotenboer J, Tsao YP. Effect of microthreads and platform switching on crestal bone stress levels: a finite analysis. *J Periodontol* 2008;79:2166-2172.

16. Schrotenboer J, Tsao YP, Kinariwala V, Wang HL. Effect of platform switching on implant crest bone stress: a finite element analysis. *Implant Dent* 2009;18:260-269.

17. Petrie CS, Williams JL. Comparative evaluation of implant designs: influence of diameter, length, and taper on stains in the alveolar crest: a three-dimensional finite-element analysis. *Clin Oral Implants Res* 2005;16:486-494.

18. Hudieb MI, Wakabayashi N, Kasugai S. Magnitude and direction of mechanical stress at the osseointegrated interface of the microthread implant. *J Periodontol* 2011;82:1061-1070.

19. Chang CL, Chen CS, Hsu ML. Biomechanical effect of platform switching in implant dentistry: a three-dimensional finite analysis. *Int J Oral Maxillofac Implants* 2010;25:295-304.

20. Hsu JT, Fuh LJ, Lin DJ, Shen YW, Huang HL. Bone strain and interfacial sliding analyses of platform switching and implant diameter on an immediately loaded implant: experimental and three-dimensional finite element analysis. *J Periodontol* 2009;80:1125-1132.

21. Streckbein P, Streckbein RG, Wilbrand JF, et al. Non-linear 3D evaluation of different oral implant-abutment connections. *J Dent Res* 2012;91:1184-1189.

22. Atieh MA, Ibrahim HM, Atieh AH. Platform switching for marginal bone preservation around dental implants: a systematic review and meta-analysis. *J Periodontol* 2010;81:1350-1366.

23. Steinebrunner L, Wolfart S, Bobmann K, Kern M. In vitro evaluation of bacterial leakage along the implant-abutment interface of different implant systems. *Int J Oral Maxillofac Implants* 2005;20:875-881.

24. Pessoa RS, Vaz LG, Marcantonio E Jr, Vander Sloten J, Duyck J, Jaecques SV. Biomechanical evaluations of platform switching in different implant protocols:

computed tomography-based three-dimensional finite element analysis. *Int J Oral Maxillofac Implants* 2010;25:911-919.

25. Yamanishi Y, Yamaguchi S, Imazato S, Nakano T, Yatani H. Influence of implant neck design and implant-abutment joint type on peri-implant bone stress and abutment micromovement: three-dimensional finite element analysis. *Dent Mater* 2012;28:1126-1133.

26. Dittmer S, Dittmer MP, Kohorst P, Jendras M, Borchers L, Stiesch M. Effect of implant-abutment connection design on load bearing capacity and failure mode of implants. *J Prosthodont* 2011;20:510-516.

27. Tabata LF, Rocha EP, Barao VA, Assuncao WG. Platform switching: biomechanical evaluation using three-dimensional finite element analysis. *Int J Oral Maxillofac Implants* 2011;26:482-491.

28. Natali AN, Pavan PG, Ruggero AL. Analysis of bone-implant interaction phenomena by using a numerical approach. *Clin Oral Implants Res* 2006;17:67-74.

29. Koo KT, Lee EJ, Kim JY, et al. The effect of internal versus external abutment connection modes on crestal bone changes around dental implants: a radiographic analysis. *J Periodontol* 2012;83:1104-1109.

30. De Almeida FD, Carvalho AC, Fontes M, et al. Radiographic evaluation of marginal bone level around internal-hex implants with switched platform: a clinical case report series. *Int J Oral Maxillofac Implants* 2011;26:587-592.

31. Ho DS, Yeung SC, Zee KY, Curtis B, Hell P, Tumuluri V. Clinical and radiographic evaluation of NobelActive™ dental implants. *Clin Oral Implants Res* 2013;24:297-304.

32. Huang B, Meng H, Piao M, Xu L, Zhang L, Zhu W. Influence of placement depth on bone remodeling around tapered internal connection implant: a clinical and radiographic study in dogs. *J Periodontol* 2012;83:1164-1171.

Table 1. Mechanical properties of bone and titanium used for finite element analysis

Component	Young' s modulus (MPa)	Poisson's ratio
Cortical bone	14,000	0.30
Cancellous bone	1,470	0.30
Titanium	116,000	0.34

Data are from Pessoa et al.[24]

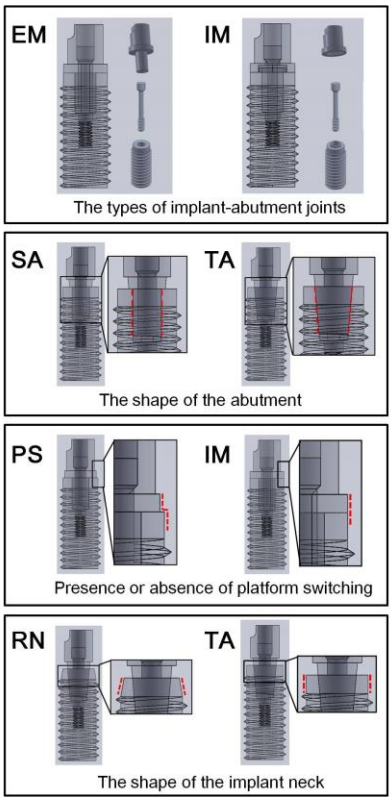

	Code					
	EM	IM	SA	TA	PS	RN
The types of implant-abutment joints	External	Internal	Internal	Conical	Internal	Conical
The shape of the abutment	Straight	Straight	Straight	Tapered	Straight	Tapered
Presence/absence of platform switching	Absence	Absence	Presence	Presence	Presence	Presence
The shape of the implant neck	Straight	Straight	Straight	Straight	Straight	Reverse conical

Figure 1. Three-dimensional computer-assisted design models. EM: external joint model; IM: internal joint model; SA: straight abutment model; TA: tapered abutment model; PS: platform switching model; RN: reverse conical neck model. For SA and TA, PS and IM, and RN and TA, the red dotted lines show the differences in the designs between models.

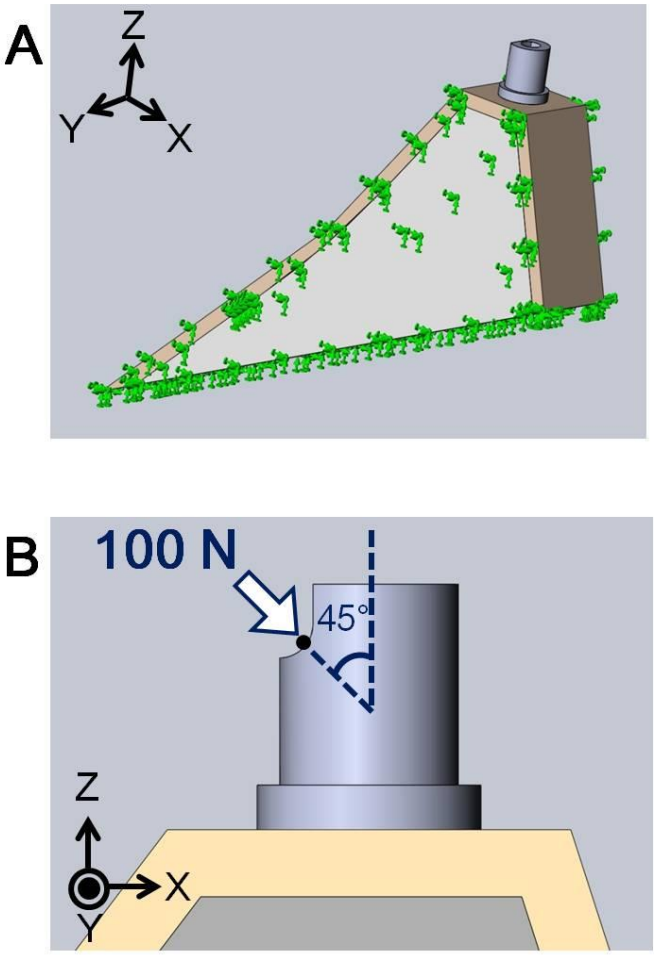

Figure 2. Implant and surrounding maxillary bone used for finite element modeling and analysis. (A) Whole assembly of bone and implant models. Green arrows show the bottom part of the bone. Both sectional surfaces of the bone segment were fixed. (B) Static load of 100 N was applied to the basal ridge surface of the abutment 45° obliquely to the long axis of the implant.

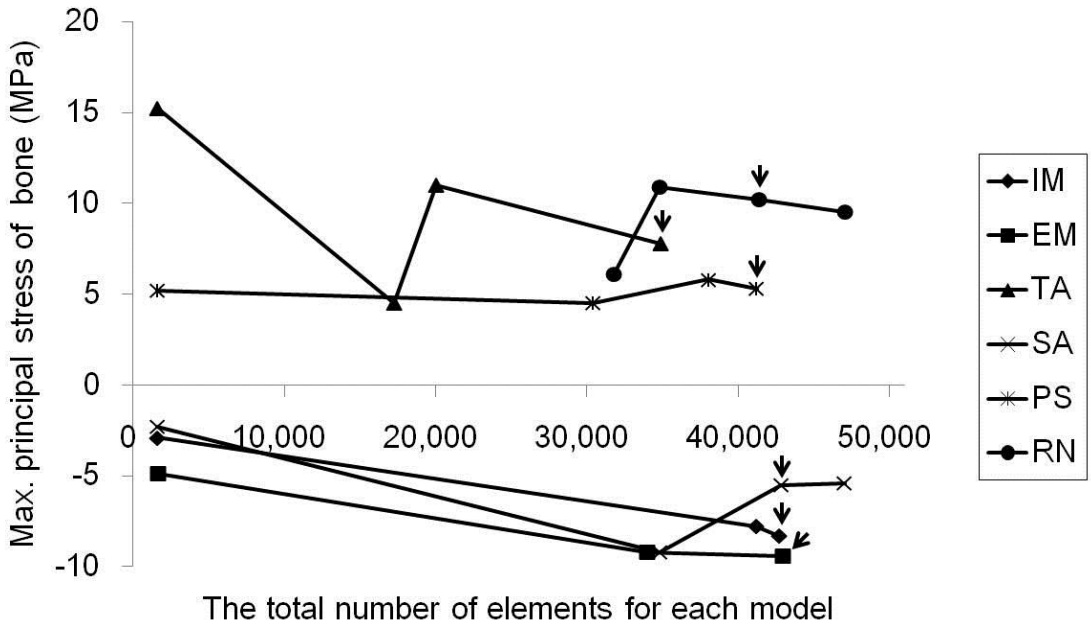

Figure 3. Results of convergence analysis in terms of maximum principal stress. Arrows point to the elements for each model at which the maximum principal stress converged.

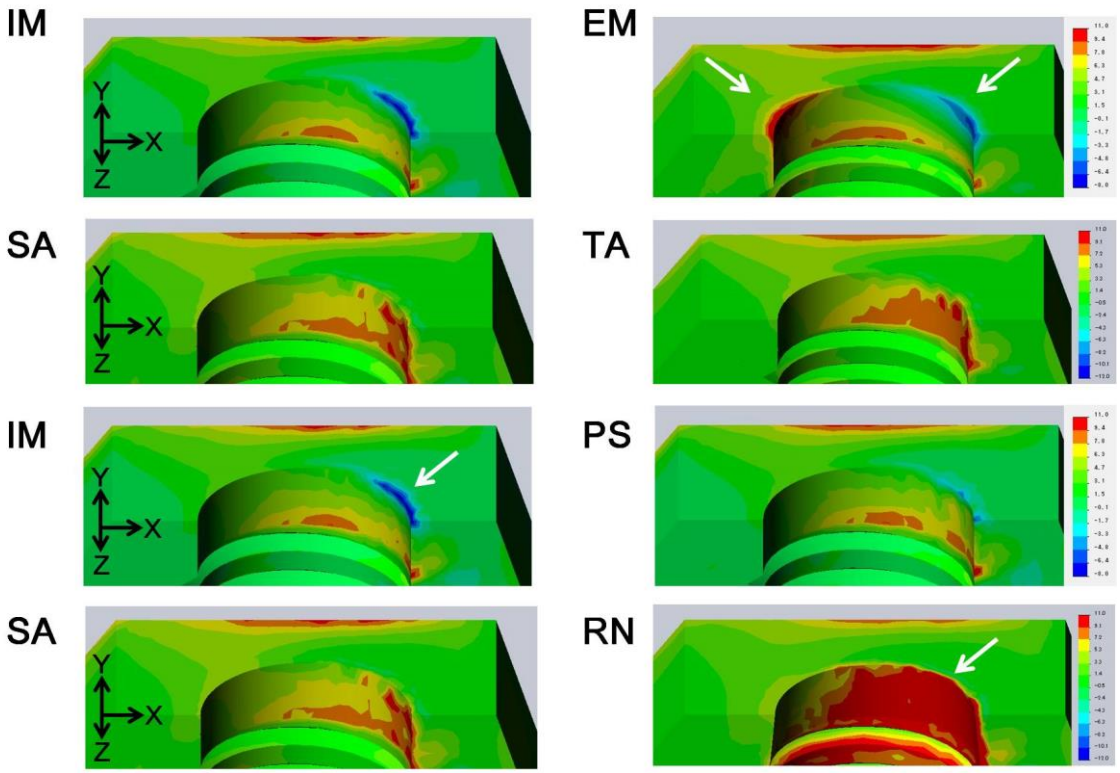

Figure 4. Distribution of the maximum principal stress. White arrows point to the concentration of the maximum principal stress.

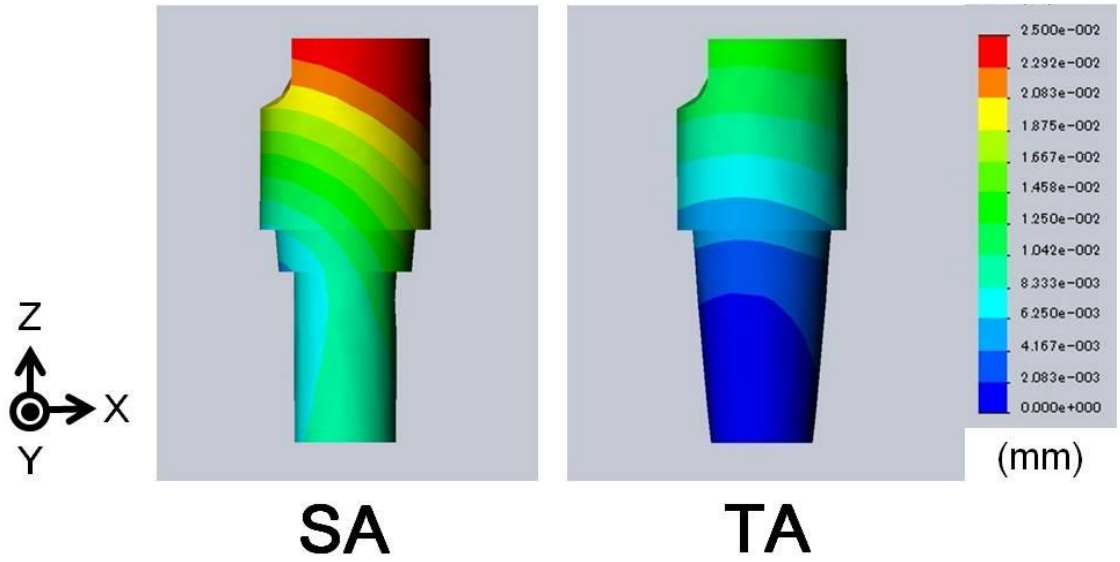

Figure 5. Distribution of abutment displacement.